33RD INTERNATIONAL COSMIC RAY CONFERENCE, RIO DE JANEIRO 2013
THE ASTROPARTICLE PHYSICS CONFERENCE

Elemental GCR Observations During the 2009–2010 Solar Minimum Period

K. A. LAVE[1], M. H. ISRAEL[1], W. R. BINNS[1], E. R. CHRISTIAN[2], A. C. CUMMINGS[3], A. J. DAVIS[3], G. A. DE NOLFO[2], R. A. LESKE[3], R. A. MEWALDT[3], E. C. STONE[3], T. T. VON ROSENVINGE[2], M. E. WIEDENBECK[4]

[1] *Washington University, St. Louis, MO 63130, USA*
[2] *NASA/Goddard Space Flight Center, Greenbelt, MD 20771, USA*
[3] *California Institute of Technology, Pasadena, CA 91125, USA*
[4] *Jet Propulsion Laboratory, California Institute of Technology, Pasadena, CA 91109, USA*

klave@physics.wustl.edu

Abstract: Using observations from the Cosmic Ray Isotope Spectrometer (CRIS) onboard the *Advanced Composition Explorer* (*ACE*), we present new measurements of the galactic cosmic ray (GCR) elemental composition and energy spectra for the species B through Ni in the energy range ∼50–550 MeV/nucleon during the record setting 2009–2010 solar minimum period. These data are compared with our observations from the 1997–1998 solar minimum period, when solar modulation in the heliosphere was somewhat higher. For these species, we find that the intensities during the 2009–2010 solar minimum were ∼20% higher than those in the previous solar minimum, and in fact were the highest GCR intensities recorded during the space age. Relative abundances for these species during the two solar minimum periods differed by small but statistically significant amounts, which are attributed to the combination of spectral shape differences between primary and secondary GCRs in the interstellar medium and differences between the levels of solar modulation in the two solar minima. We also present the secondary-to-primary ratios B/C and (Sc+Ti+V)/Fe for both solar minimum periods, and demonstrate that these ratios are reasonably well fit by a simple "leaky-box" galactic transport model that is combined with a spherically symmetric solar modulation model.

Keywords: cosmic rays, Galaxy: abundances, Sun: activity

1 Introduction

Solar modulation in the heliosphere distorts the interstellar composition and energy spectra of inwardly diffusing galactic cosmic ray (GCR) nuclei. Those nuclei with interstellar energies less than a few GeV/nucleon suffer significant energy loss due to adiabatic deceleration. During solar minimum periods of the ∼11 year solar cycle, these losses are minimized.

In the solar system, observations during solar minima give us the best opportunity to study GCR nuclei close to interstellar medium (ISM) conditions. This information can provide insight to interstellar transport processes, which then yield better estimates for the GCR source composition. The most recent solar minimum period, which occurred between 2007–2010, exhibited very low levels of solar activity. Observations made during this time are therefore the closest we have come near Earth to observing GCRs in ISM conditions.

The Cosmic Ray Isotope Spectrometer (CRIS, [1]) on board NASA's *Advanced Composition Explorer* (*ACE*) has been continuously observing GCR nuclei arriving near Earth since its launch on 25 August 1997. Using high statistics observations from CRIS, we present the elemental energy spectra and composition of boron through nickel ($5 \leq Z \leq 28$) in the energy range ∼50–550 MeV/nucleon. Data were obtained from a 297-day period from 2009 March 23 to 2010 January 13, which is characterized as having the highest GCR intensities of the space era [2]. These results are compared with observations from the 1997–1998 solar minimum period [3], covering data from 1997 December 5 to 1998 April 19, which exhibited somewhat higher levels of solar modulation. Additionally, we present the B/C and (Sc+Ti+V)/Fe ratios for both solar minimum periods, and demonstrate that a "leaky-box" interstellar transport model combined with a spherically symmetric solar modulation model is able to give reasonably good fits to the observed ratios.

2 CRIS Instrument

The CRIS instrument consists of four silicon solid-state-detector (SSD) stacks; in each stack, fifteen circular SSDs are grouped into nine individual detectors (E1–E9; see Figure 1). A scintillating optical fiber trajectory (SOFT) hodoscope positioned above the stacks is used to determine the trajectories of incident particles. The hodoscope is composed of three *x*–*y* tracking layers, with an additional set of layers serving as a trigger. For a particle stopping in the silicon detectors, the charge, mass, and incident energy at the top of the instrument are determined using the total energy deposited (*E'* in MeV) in the detector in which the particle stopped and multiple measurements of the rate of energy loss (*dE/dx* in MeV g^{-1} cm^2) in the other detectors through which it passed. For a more detailed description of the CRIS instrument, see [1] and [4].

Events used in this analysis were those produced by nuclei that have incident angles $\leq 30^\circ$ from the normal that stopped in the active areas of detectors E2–E8. The bottom detector (E9) in each stack is used to eliminate those particles that do not stop in the preceeding detectors or that interact and produce one or more long-range fragments. Additionally, particles must not have a calculated stop depth

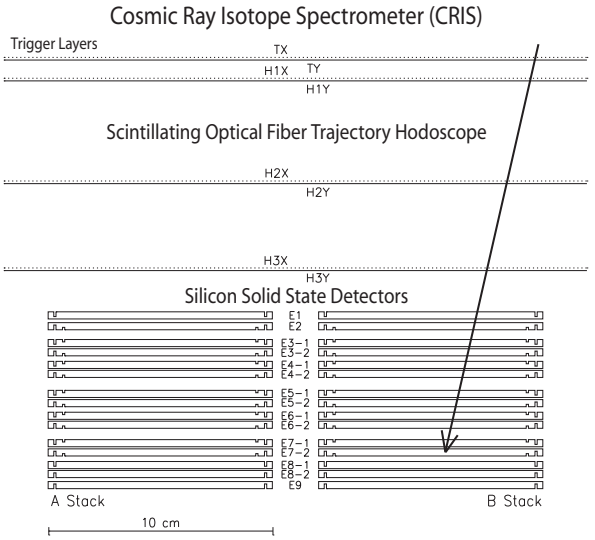

Figure 1: CRIS instrument cross section (two of the four detector stacks shown). The arrow represents an incident particle stopping in the bottom of detector E7.

within 160 μm of the top or bottom face of the detector to avoid complications in interpreting energy losses for particles that stop near surface "dead layers" in the detector.

3 Elemental Spectra

Elemental intensities for boron through nickel ($5 \leq Z \leq 28$) are determined for seven energy bins corresponding to GCRs stopping in detectors E2–E8 of the CRIS instrument. Figure 2 shows the energy spectra for the 2009–2010 solar minimum period, where we have applied energy-independent scale factors to the data to allow for an easy comparison between the spectral shapes. The spectra have been corrected for livetime, geometrical acceptance of the instrument, energy intervals, fragmentation in the instrument, and hodoscope efficiencies. Plotted uncertainties are the quadratic sum of the statistical and systematic contributions. The vertical dotted line at 160 MeV/nucleon shows that there is a common energy at which CRIS is sensitive to all the species considered here.

Figure 3 compares selected CRIS primary element spectra (carbon, oxygen, silicon, and iron) from the 1997–1998 [3] and 2009–2010 solar minimum periods. For all four species, the data are plotted at the mid-point energies of each energy interval. We see that at each energy, the 2009–2010 intensities are $\sim$20% higher than those from the 1997–1998 solar minimum. In Figure 4, we show that most of the elements between boron ($Z = 5$) and nickel ($Z = 28$) have an $\sim$20% increase in intensity for 2009–2010 as compared to 1997–1998.

4 Composition

Relative elemental abundances are calculated by first fitting parabolas in log(Intensity) versus log(Energy/nucleon) to the energy spectra, as shown in Figure 2. We then take ratios of the curves at the common energy, 160 MeV/nucleon, to determine the relative abundances.

Table 1 gives the 1997–1998 and 2009–2010 CRIS solar minimum relative abundances. The values have been

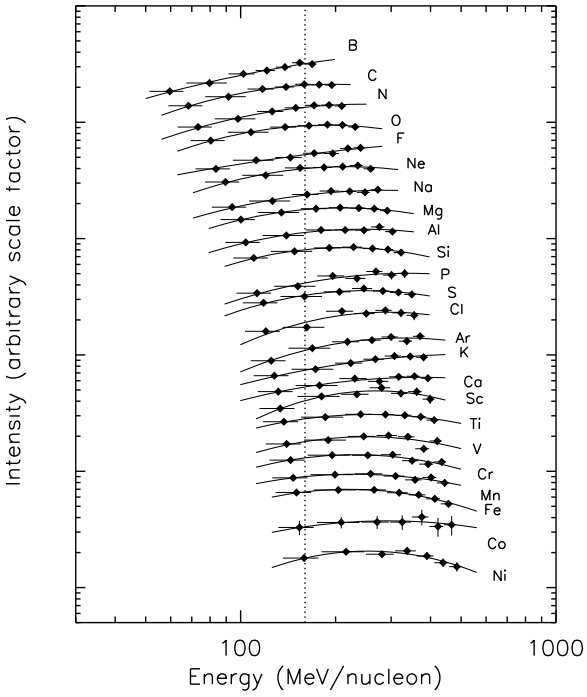

Figure 2: CRIS elemental spectra for the 2009–2010 solar minimum. Energy-independent scale factors have been applied to the data to allow for easy comparison of the spectral shapes. The solid lines are quadratic fits to the data, which are used to determine the relative abundances at 160 MeV/nucleon (indicated by the vertical dotted line).

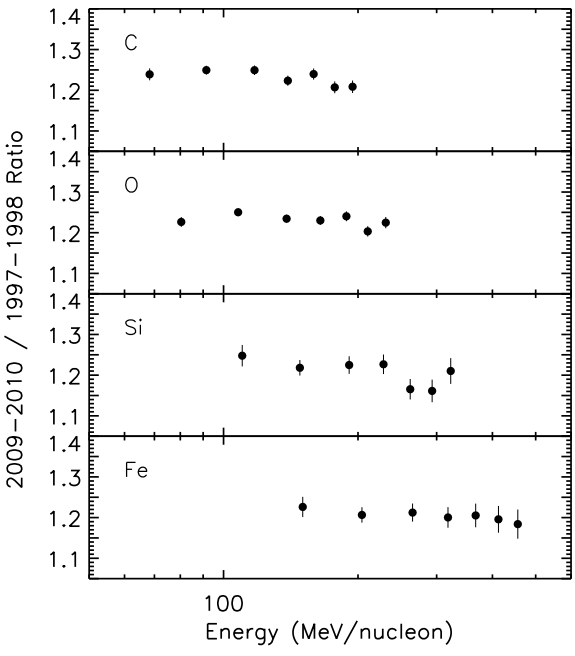

Figure 3: Comparison of the CRIS primary element spectra for the 1997–1998 and 2009–2010 solar minima. Only statistical uncertainties are shown.

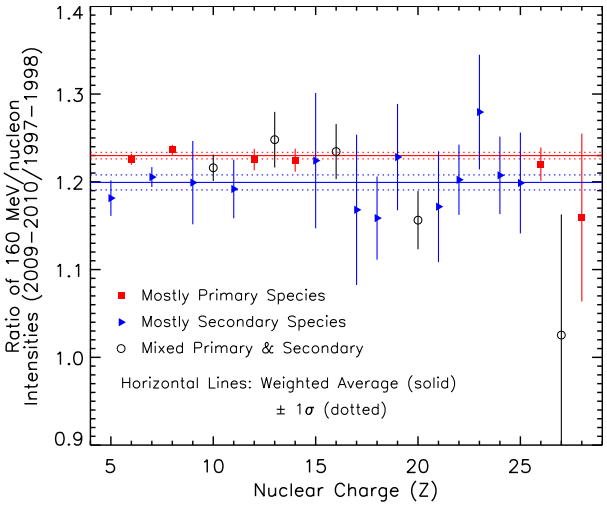

Figure 4: Ratio of the 2009–2010 solar minimum intensities at 160 MeV/nucleon relative to the 1997–1998 intensities. Species that are mostly primary are given as filled red squares, while species that are mostly secondary are given as filled blue triangles; species that have significant primary and secondary components are given as open black circles. Only statistical uncertainties are shown. The weighted averages of the ratios for the primary (solid red horizontal line) and secondary (solid blue horizontal line) species are shown; the dotted lines give the 1σ uncertainties on each average.

CRIS Relative Elemental Abundances At 160 MeV/nucleon		
Element	**1997–1998**	**2009–2010**
B	1788.6± 30.1	1725.7± 19.4
C	7227.0± 73.3	7235.4± 45.0
N	1705.2± 20.9	1678.9± 12.3
O	7067.2± 70.9	7137.0± 42.7
F	99.4± 3.5	97.3± 2.1
Ne	1005.5± 14.1	998.9± 8.4
Na	190.3± 4.9	185.2± 2.9
Mg	1374.3± 17.3	1375.3± 10.3
Al	199.4± 4.7	203.2± 2.8
Si	1000.0± 13.0	1000.0± 7.8
P	26.7± 1.5	26.7± 0.9
S	155.7± 3.7	157.0± 2.2
Cl	26.0± 1.7	24.8± 0.8
Ar	58.4± 2.1	55.3± 1.2
K	39.9± 1.7	40.1± 1.0
Ca	126.5± 3.3	119.5± 1.9
Sc	26.4± 1.1	25.3± 0.9
Ti	102.3± 3.1	100.5± 1.8
V	46.0± 2.1	48.1± 1.3
Cr	100.2± 3.3	98.8± 1.9
Mn	63.3± 2.7	61.9± 1.6
Fe	673.7± 10.9	671.4± 6.5
Co	4.4± 0.3	3.7± 0.4
Ni	31.6± 2.2	29.9± 1.3

Table 1: Values are normalized to Si≡1000. Only the statistical uncertainties are given. The absolute intensities (with combined statistical and systematic uncertainties) for silicon at 160 MeV/nuc are $(108.2 \pm 3.4) \times 10^{-9}$ (cm^2 s sr MeV/nuc)$^{-1}$ for 1997–1998 and $(132.5 \pm 4.1) \times 10^{-9}$ (cm^2 s sr MeV/nuc)$^{-1}$ for 2009–2010.

normalized to Si≡1000, and only statistical uncertainties are given. The differences between the relative abundances for the two solar minima are small, but nevertheless statistically significant, as illustrated in Figure 4.

Solar modulation in 2009–2010 was lower than in 1997–1998, so the GCRs CRIS observed in 2009–2010 had lower interstellar energies. At CRIS energies, lower-energy particles traverse less material in the Galaxy, on average, resulting in the production of fewer secondary species (those produced by fragmentation in the ISM). This is consistent with the results in Figure 4. Species that are considered to be mostly primary material from the source are shown as red squares, while species that are mostly secondary material are given as blue triangles. The horizontal solid lines show the average ratios of the intensities for the primary (red) and secondary (blue) species, weighted by the statistical uncertainties of the ratios. The horizontal dotted lines are the 1σ uncertainties on the weighted averages. We note that the species which have significant primary and secondary components (open black circles) are not used when computing the averages. Although the 2009–2010 intensities are higher than those in 1997–1998, the secondary species do not show as large of an increase as the primary species in 2009–2010, compared with 1997–1998.

5 Secondary-To-Primary Ratios

The secondary-to-primary ratios B/C and (Sc+Ti+V)/Fe are commonly studied to test interstellar transport models. These ratios are less sensitive to the source spectrum and the solar modulation model than the energy spectra, and they probe the amount of material that GCRs traverse in the ISM before escaping from the Galaxy.

In Figure 5 we show the CRIS B/C and (Sc+Ti+V)/Fe ratios for the 1997–1998 and 2009–2010 solar minima (red circles and blue diamonds, respectively). Additional measurements from other experiments are shown at energies above 400 MeV/nucleon (HEAO: [5], TRACER: [6], CRN: [7], ATIC-2: [8], AMS-01: [9], CREAM: [10]). Also shown are the ratios calculated from our transport model [4, 3], which uses a steady-state "leaky-box" interstellar model combined with the spherically-symmetric Fisk model for solar modulation [11]. We have characterized the levels of solar modulation using the "modulation potential" ϕ, with values of 325 MV and 250 MV for the 1997–1998 and 2009–2010 solar minima, respectively.

Characteristic maxima in both the data and the models are seen near ∼1 GeV/nucleon for both ratios. These ratios correspond to the distribution of path lengths that GCRs observed near Earth traversed in the Galaxy. At higher energies the ratios decrease with increasing energy because higher-energy GCRs escape more easily from the Galaxy. At lower energies the ratios increase with increasing energy; this indicates there is a depletion of path lengths at low energies [12, 13, 14, 15].

Above ∼1 GeV/nucleon, where the effects of solar mod-

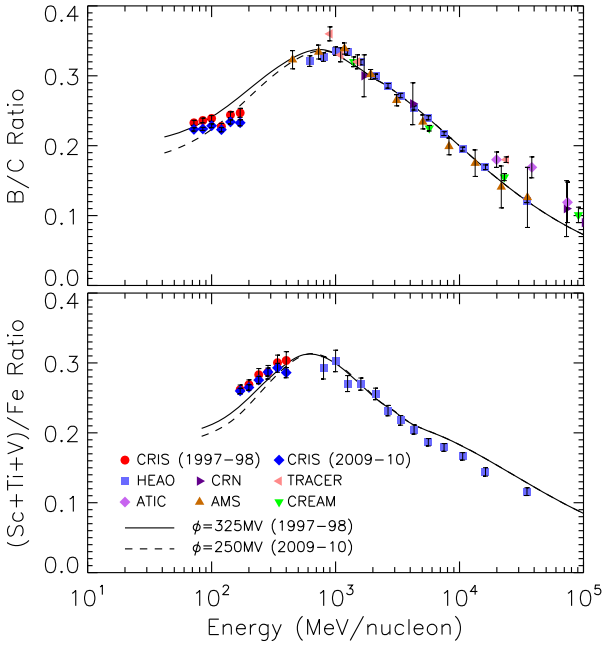

Figure 5: CRIS B/C and (Sc+Ti+V)/Fe ratios for 1997–1998 and 2009–2010 (red circles and blue diamonds, respectively). For references to the other data, see Section 5. The solid and dashed curves are the result of our transport model using modulation values of 325 MV (1997–1998) and 250 MV (2009–2010), respectively.

ulation become negligible, the B/C ratio is well fit by the model. At CRIS energies, the models for both solar minimum periods have stronger energy dependences than the data, which are observed to have relatively flat shapes. The differences between the models and the data are, on average, 5% and 6% for the 1997–1998 and 2009–2010 solar minima, respectively.

Both models have approximately the right shape for the (Sc+Ti+V)/Fe ratios, though the observed ratios at CRIS energies are slightly underestimated. For the 1997–1998 solar minimum the model is ∼5% lower than the data, while it is ∼7% lower than the observed 2009–2010 ratio. Above ∼5 GeV/nucleon there are similar difficulties fitting the data, which are somewhat overestimated by the model.

While small adjustments to the modulation values (±25 MV) can help us better fit the low-energy B/C ratios, the (Sc+Ti+V)/Fe ratio is quite insensitive to small changes in the modulation value [3]. Additional measurements of nuclear fragmentation cross sections are needed to further improve our model results.

6 Conclusions

We have presented the elemental energy spectra and relative abundances for the GCR species boron to nickel during the recent 2009–2010 solar minimum period using the CRIS instrument. Compared with CRIS observations from the 1997–1998 solar minimum, we see that the 2009–2010 GCR intensities increased by ∼20%. The relative elemental abundances are similar in both time periods, but do exhibit small differences associated with the differing solar modulation levels in conjunction with differences in spectral shape between primary and secondary species. The secondary-to-primary ratios B/C and (Sc+Ti+V)/Fe are also shown for both time periods, and we have demonstrated that a "leaky-box" interstellar transport model combined with a spherically symmetric solar modulation model gives a reasonable fit to both ratios.

Acknowledgements

This research was supported by NASA at Caltech, Washington University, JPL, and GSFC under grants NNX08AI11G and NNX10AE45G.

References

[1] E. C. Stone, et al. , Space Sci. Rev., 86, 285, (1998).
[2] R. A. Mewaldt, et al. , ApJ, 723, L1, (2010).
[3] K. A. Lave, et al. , submitted to ApJ, (2013).
[4] J. S. George, et al. , ApJ, 698, 1666, (2009).
[5] J. J. Engelmann, et al. , Astron. & Astrophys., 233, 96, (1990).
[6] A. Obermeier, et al. , ApJ, 742, 14, (2011).
[7] S. P. Swordy, et al. , ApJ, 349, 625, (1990).
[8] A. D. Panov, et al. , 30th Internat. Cosmic Ray Conf., 2, 3, (2008).
[9] M. Aguilar, et al. , ApJ, 724, 329, (2010).
[10] H. S. Ahn, et al. , Astropart. Phys., 30, 133, (2008).
[11] L. A. Fisk, JGR, 76, 221 (1971).
[12] M. Garcia-Muñoz, et al. , ApJ Supp., 64, 269, (1987).
[13] K. E. Krombel & M. E. Wiedenbeck, ApJ, 328, 940, (1988).
[14] A. J. Davis, et al. , AIP Conf. Ser., 528, 421, (2000).
[15] N. E. Yanasak, et al. , ApJ, 563, 768, (2001).